

Simulation of Flow Field and Particle Trajectories in Hard Disk Drive Enclosures

H. Song*, M. Damodaran* and Quock Y. Ng**

*Singapore-Massachusetts Institute of Technology Alliance (SMA)
Nanyang Technological University, Nanyang Avenue, Singapore 639798

**Seagate Technology International
63 The Fleming, Science Park Drive, Singapore Science Park, Singapore 118249

Abstract — The airflow field and particle trajectories inside hard disk drive (HDD) are investigated in this study using commercial software *Fluent* and *Gambit*. Three-dimensional grids inside the HDD configuration are built using *Gambit* taking into account all the components and their geometric details. The airflow field inside HDD is simulated using three incompressible Navier-Stokes equations for various disk rotational speeds. The effects of using the various turbulence models inside the *Fluent* software such as the standard $k-\epsilon$, RNG $k-\epsilon$ and Reynolds Stress Method on the computed airflow characteristics are also assessed. Steady flow fields and the effects of rotational speeds are assessed. Based on the computed steady airflow patterns, particle trajectories are computed using routines available in *Fluent* as well as special particle trajectory functions defined by the user via the user-defined functions. Particles of different sizes and materials are injected at various locations in the computed flow field and the corresponding particle trajectories are studied. Based on the investigation, the trajectory tends to be different according to sizes and materials. The present work forms a basis for further investigation of heat transfer processes inside the HDD to address thermal management issues and also the computation of unsteady flow fields in the HDD due to the movement of the actuator arm during data storage and retrieval

Index terms: Hard Disk Drives (HDD), Computational Fluid Dynamics (CFD), Particle Trajectories; Fluent CFD Software

Manuscript received October 31, 2003. This work was supported in part by Seagate Technology Int'.

Hanbing Song, is with the Singapore-MIT Alliance, N2-B2-C15, 50 Nanyang Ave, Nanyang Technological University, 639798, Singapore (e-mail: g0200727@nus.edu.sg).

Murali, Damodaran, is an Associate Professor with the School of Mechanical and Production Engineering, Nanyang Technological University and a SMA Fellow (Phone: 65-67905599, e-mail: mdamodaran@ntu.edu.sg).

Quock Y. Ng is Principal Engineer with the Seagate Technology Int' (e-mail: Quock.Y.Ng@seagate.com).

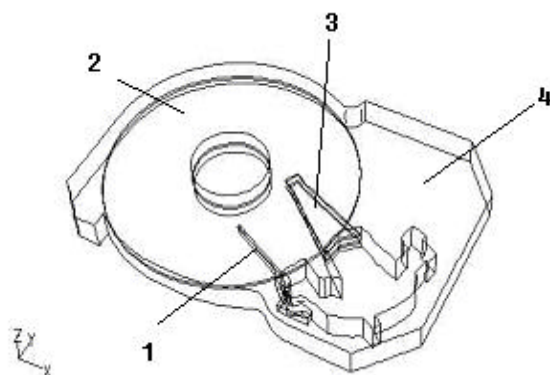
I. INTRODUCTION

THE hard disk drive is one of the most important components in many computers these days and it is the primary device, which provides storage space for soft wares and data. In today's hard disk drive industry, the demand for higher recording density and higher rotating speed has become more and more stringent and this requires a good understanding of the airflow characteristics to achieve a highly accurate head positioning. At the same time, high-speed disk rotation causes high-speed airflows in the HDD, which in return affects the head positioning accuracy. Additionally, particles inside a HDD can cause performance degradation to the HDD via processes such as chemical erosion, scratch, etc, which may lead to inaccurate reading and writing of data or un-correctable error. The degree of performance degradation depends on the type and size of the particles. As the number of bits of data per area increases, the severity of the damage caused by a given particle increases. Thus, the removal of particles from inside a HDD is increasingly demanding. Knowledge of flow dynamics is essential for designing an efficient particle removal system. The particle trajectories inside the HDD could be visualised experimentally using instruments such as PIV (Particle Image Velocimetry) and other techniques outlined in Bhushan et al. [1]. Airflow induced vibration of components in the HDD are also important for ensuring the overall integrity of the HDD. Ma et al. al [2] has addressed issues concerning the friction and wear behaviour of major particles inside HDD this suggests that it is important to know the particle trajectories inside the HDD during the disk operation so that efficient particle filter systems could be designed to keep particle induced performance degradation to a minimum. Since the experimental work for understanding all these phenomena have their own limitations, computational simulation using modern numerical methods for solving fluid flow in the HDD offers an alternative path for investigating these issues. In fact there have been several attempts at the numerical simulation for airflow in HDD. Wu et al. al [3] used multi-grid numerical schemes on unstructured triangular meshes to

numerically solve the slider air-bearing problem of hard disk drives for fixed slider attitude. Tatewaki et al [4] has investigated the mechanisms causing disk flutter in hard disk drives, and simulated the dynamics in a HDD with three stacked disks, using the LES model of turbulence. This paper is mainly focused on the numerical simulation of airflow and the particle trajectories inside a commercial HDD enclosure using *Fluent* [5] and *Gambit* [6].

II. MODEL OF HARD DISK DRIVE

The commercial HDD used in this study for the investigation of airflow characteristics and particle trajectories is shown in Fig. 1.



1-Air Latch; 2-Disk; 3-Arm; 4-Base

Fig. 1: HDD Model

The major components are the air latch, disk, arm and base as indicated in the figure. During operation, the disk will rotate at a specified rotating speed, which is typically greater than 5400 revolutions per minute (rpm). The arm will also move for data storage and retrieval purposes. The space inside the HDD where the airflow is to be characterised is discretized with unstructured meshes using *Gambit*. The computation of flow fields in this space is then done using *Fluent* by specifying the appropriate boundary conditions on all solid surfaces and on the disk surface, which rotates at a specific RPM. The flow is computed to reach a steady state. To enable flow visualization during post processing, three cutting planes and two lines are created to display contours of computed flow patterns to delineate flow structures and the location and orientation of these planes relative to the coordinate system are shown in Fig. 2.

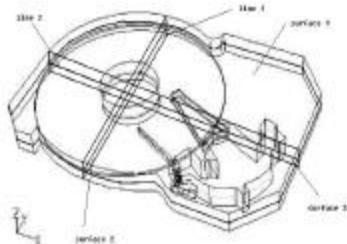


Fig. 2: Cutting Planes and Lines (3D view)

All these surfaces and lines are chosen to have a representative snapshot of the flow structure at the critical areas of interest. Surface 1 is located between the disk and the diverter and is about 0.0104m from the bottom of the base. Surfaces 2 and 3 are two planes through the hub or imaginary centre of the rotating disk. Line 1 is the intersection of surfaces 1 and 2 while line 2 is the intersection of surfaces 1 and 3.

III. COMPUTATION OF AIRFLOW CHARACTERISTICS IN HDD

Airflow characteristics in the HDD enclosure are computed by solving the unsteady incompressible Navier-Stokes Equations. Three turbulence models, i.e. the Standard $k - \epsilon$, RNG $k - \epsilon$ and Reynolds Stress Method (RSM) models are implemented in the computational of flow for the disk rotating at a specified rotational speed on the same computational grid that discretizes the airflow domain inside the HDD. TABLE I shows the convergence of the flow algorithm to steady state for the computation of steady flow inside the HDD, using the three turbulence models.

TABLE I
CONVERGENCE TIME PERFORMANCE
FOR DIFFERENT TURBULENT MODELS

	Convergence Criteria	Iterations	Time taken
Standard $k - \epsilon$	10^{-5}	1623	20 hours
RNG $k - \epsilon$	10^{-5}	1810	24 hours
RSM	10^{-3}	1985	36 hours

Standard and RNG $k - \epsilon$ are both solved till the convergence criteria of 10^{-5} is satisfied. It can be seen that the RNG $k - \epsilon$ takes more iterations and time to converge than the standard $k - \epsilon$. As for RSM, even though the convergence criterion is set to 10^{-3} , which is less restrictive than the other two, it costs more iterations and time than the other two. It is reasonable because in standard $k - \epsilon$ model, only two turbulence transport equations are solved. The extra terms and functions in the governing equations and a greater degree of non-linearity in RNG $k - \epsilon$ model takes a little bit longer time to converge. It appears that RSM is the most expensive model because it has to solve seven additional equations. The $k - \epsilon$ can satisfy the more stringent convergence criteria in less time and fewer iterations. Plots of the computed velocity and static (gauge) pressure contours on surface 1 (top) appear indistinguishable for all three turbulence models. A typical plot of these contours is shown in Fig. 3.

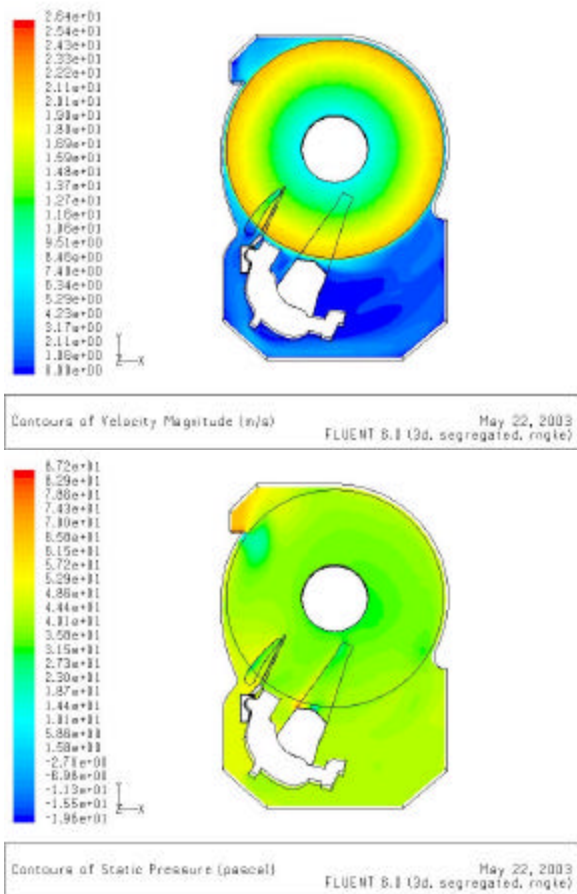


Fig. 3: Velocity (upper) and Pressure (below) Contours on a plane near the top disk surface

From these plots it can be observed that the airflow velocities increase from the ID (Inner Diameter) to the OD (Outer Diameter) of the disk. The velocity then drops as one moves away from the OD of the disk, toward the cavity of the HDD (bottom of Fig. 3, left). Fig. 3, upper, shows the airflow velocity reaches a maximum value of 26.4m/s @ the OD of disk. The tangential velocity increases linearly in the radial direction, from ID to OD of the disk. Fig. 3, below, shows the pressure is highest at the top left where the re-circulation filter is located. At this point, airflow encounter an obstacle, it slows down quickly while the pressure builds up correspondingly. The pressure decreases away from this region and at locations adjacent to the diverter and the actuator arm. Fig. 4 provides a side view of the velocity contours, in the z-direction. It represents Surface 2 of Fig. 2, showing the velocity is highest close to, and toward the OD of the disk surface; lowest away from it.

Fig. 5 shows the variation of the magnitude of the velocity along the Lines 1 (Surface 2) near to the disk surface and this variation conforms to the expected variation from the physical point of view. The magnitude of the velocity increases linearly along the disk surface, from ID to OD, then drops sharply at points toward the cavity of the HDD (Surface 1 of Fig. 2). In the vicinity of the various components such as the actuator arm and so on, the variation of the magnitude of the velocity along the line is not linear.

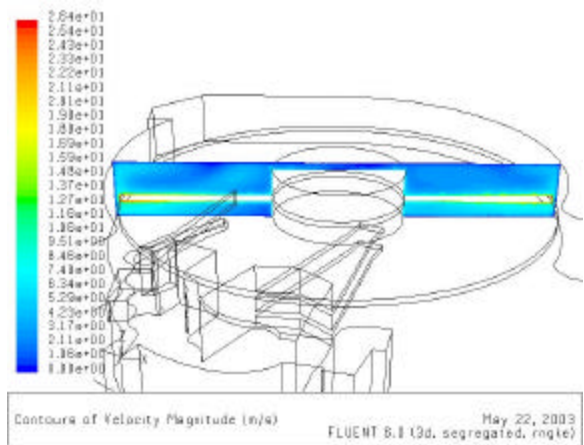


Fig. 4: Side View of Velocity Contours on a Selected Plane

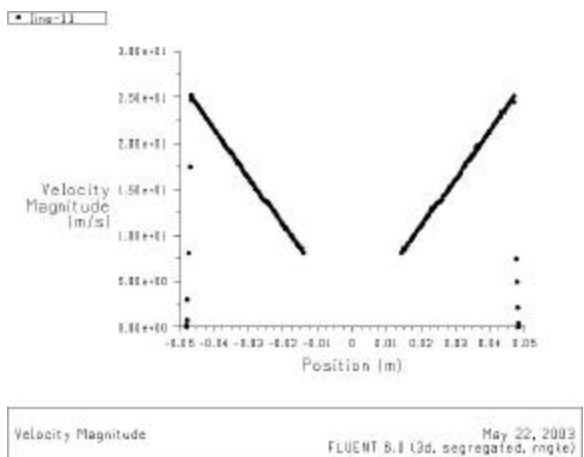


Fig. 5: Variation of Velocity along Selected Lines at Selected Locations

Fig. 6 shows plot of the velocity vectors on a selected Z-X plane. The occurrence of a pair of vortices can also be seen in the upper and lower spaces, respectively thereby giving useful insight into the flow structures that develop in the confined spaces of the HDD and enable an elucidation of the flow physics.

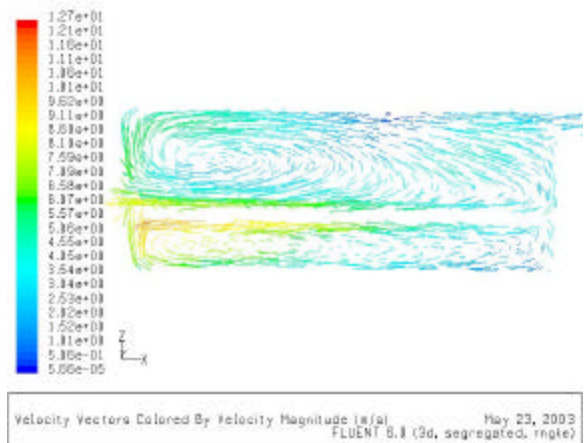
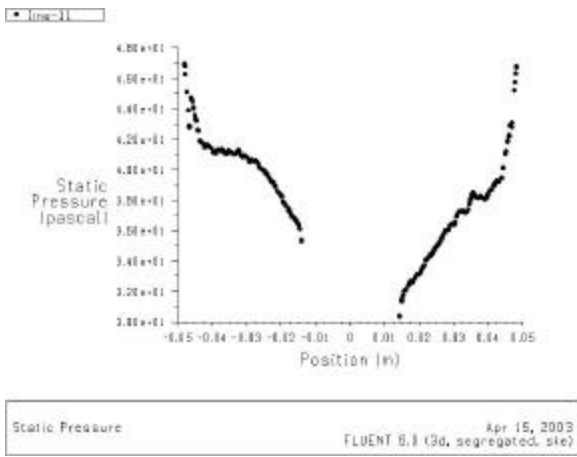
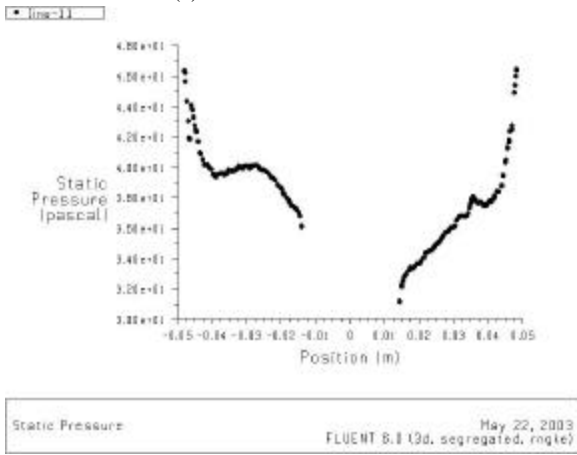


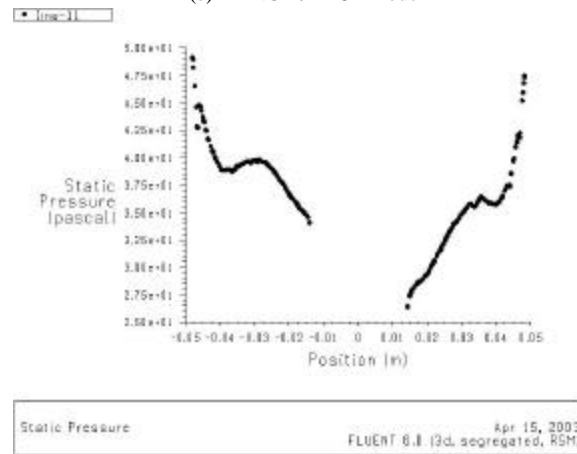
Fig. 6: Velocity Vector Plots on a selected Z-X plane



(a) Standard $k - e$ Model

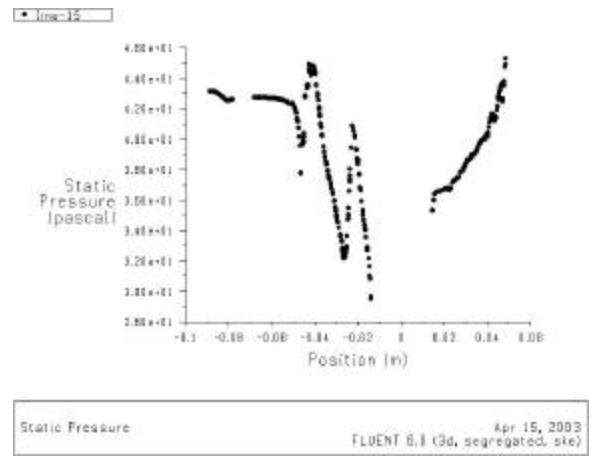


(b) RNG $k - e$ Model

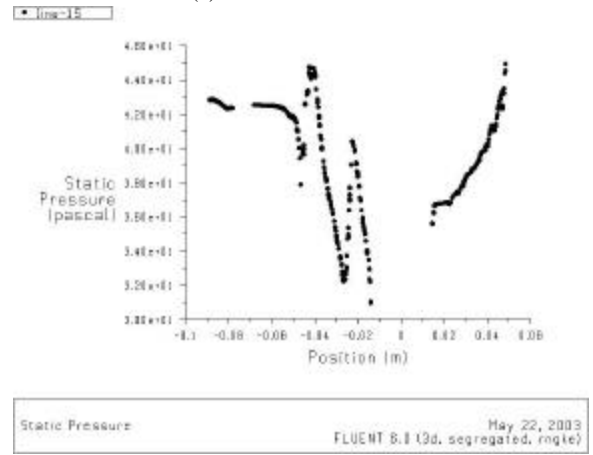


(c) Reynolds Stress Method (RSM)

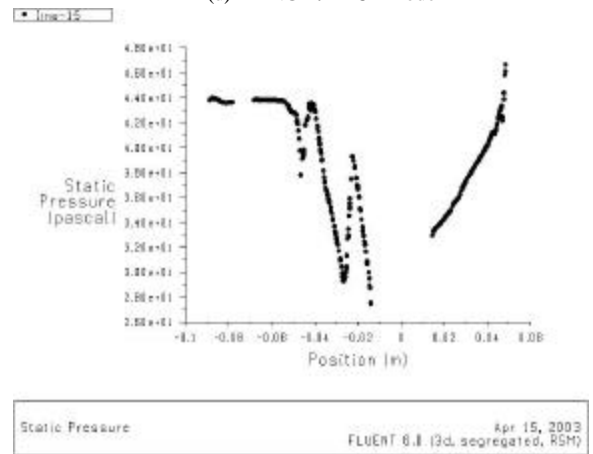
Fig. 7: Static gauge pressure variation along line 1 on surface 2 as predicted by the simulation using different turbulence models



(a) Standard $k - e$ Model



(d) RNG $k - e$ Model



(e) Reynolds Stress Method (RSM)

Fig. 8: Static gauge pressure variation of along line 2 on surface 3 as predicted by the simulation using different turbulence models

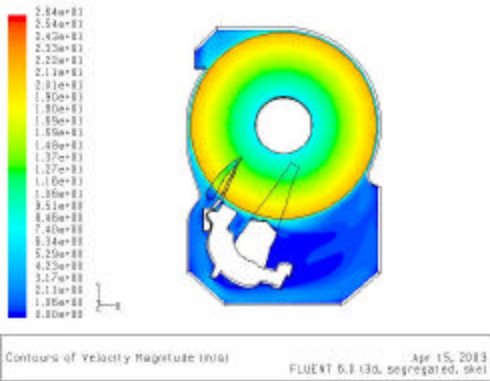
Although the static gauge pressure contours computed by using the three turbulence models appear to be similar, examination of the computed values show some minor differences. For example the maximum value of the static gauge pressure ranges in values from 88.8 pa, 87.2pa and 84.9pa for the RSM, the RNG $k - e$, and standard $k - e$, respectively. Fig. 7 shows the variation of the static gauge pressure along line 1 on surface 2, which is a line on the plane close to the disk surface, for the three turbulence models. It

can be seen that the RSM turbulence model gives a greater value compared with the other two $k - \epsilon$ methods. Along line 1 over the domain ranging from $s = -0.044$ to $s = -0.026$, (s is measured from the centre of the disk radially outward) the predicted variation using the standard $k - \epsilon$ decreases monotonically. However, the predictions using the RNG $k - \epsilon$ and RSM increase first, reach the peak at $s = -0.026$, and then decrease. Fig. 8 shows the variation of the static gauge pressure along line 2 on surface 3, which is a plane close to the disk surface. Although the plots are similar, the values predicted using the RSM turbulence model shows higher values. It appears that in the left part of the side-view disk, the static gauge pressure value calculated using RSM turbulence model is greater than that calculated using the $k - \epsilon$ model. The predictions from the two $k - \epsilon$ turbulence models follow the same pattern.

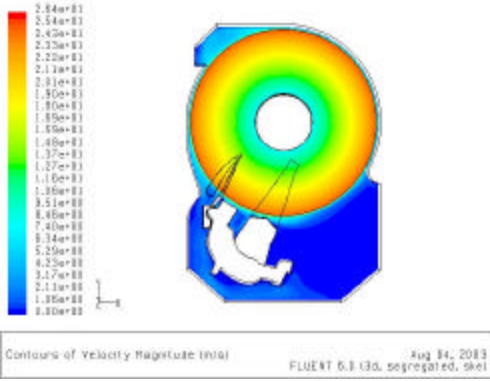
Theoretically the RSM model should be more accurate than $k - \epsilon$, because it solves seven additional equations. However computationally it is slow to converge as compared with computations using the $k - \epsilon$ turbulence models. Based on the observations of computed solutions RNG $k - \epsilon$ could be a preferred choice than the standard $k - \epsilon$ model for the problem of airflow simulation in HDD. However much depend on the comparison of the shear stress patterns on the disk, wall and component surfaces with experimental measurements before one could make any conclusive statements on the proper choice of turbulence model for this simulation.

By comparing the convergence trends of the computations using the three turbulence models, it is noted that when the disk rotation is moved to 7200RPM, the computation using RNG $k - \epsilon$ turbulence model appear to have flatten out before satisfying the specified convergence criteria of 10^{-5} order of reduction in the residuals. This could be due to possible flow instabilities caused by higher rotational speed. However, standard $k - \epsilon$ did converge to the given criteria of 10^{-5} quickly. At higher rotational speeds, more iterations are required to reach the specified tolerance limit for convergence.

Thermal effects on the global air flow characteristics inside the HDD are considered by treating the spindle motor as one of the main heat source inside HDD and the outer surface of the HDD as being subjected to a fixed temperature. The flow and energy equations are then solved and contours of velocity and pressure fields examined for the case of the disk spinning at 5400 rpm. It is found that while the thermal effects resulting from the specified heat sources do not alter the maximum value of the velocity magnitude, they have an effect of the re-distribution of the velocity field and pressure field in the HDD as could be seen on a selected plane shown in Fig 9 and 10.

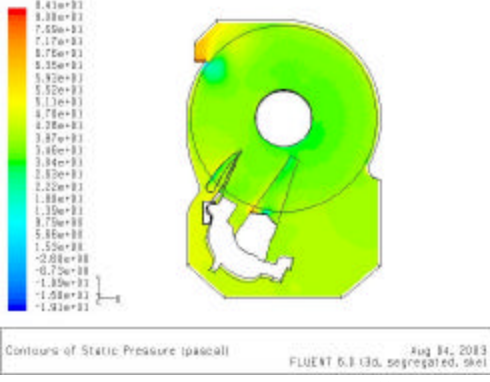


(a) Simulation without Thermal Effects

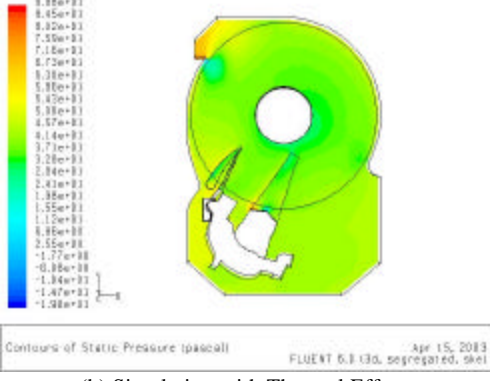


(b) Simulation with Thermal Effects

Fig. 9: Thermal Effects on Velocity Field Contours (5400RPM)



(a) Simulation without Thermal Effects



(b) Simulation with Thermal Effects

Fig. 10: Thermal Effects on the Static gauge Pressure (5400RPM)

IV. PARTICLE TRAJECTORIES

The motivation for tracking particle trajectories in the HDD enclosure is to minimize particle-induced damage. Titanium and polystyrene, representing ‘hard’ and ‘soft’ particles, were used for the initial simulation. Using the converged numerical flowfield inside the HDD, computed by the $k - \epsilon$ model, three particles of different sizes (diameter = 0.1um, 0.3um and 0.5um) for titanium and polystyrene, are injected at three different locations near the inner diameter (ID), mid diameter (MD) and outer diameter (OD), respectively. The particle trajectories are then tracked using the particle force balance model and particle trajectory integration schemes available in *Fluent* using the computed flow field to supply the necessary information into this trajectory model. The computed trajectories of titanium and polystyrene particles from their initial locations to their final position are shown in Fig. 11 and Fig. 12 for the rotating speed of 5400RPM.

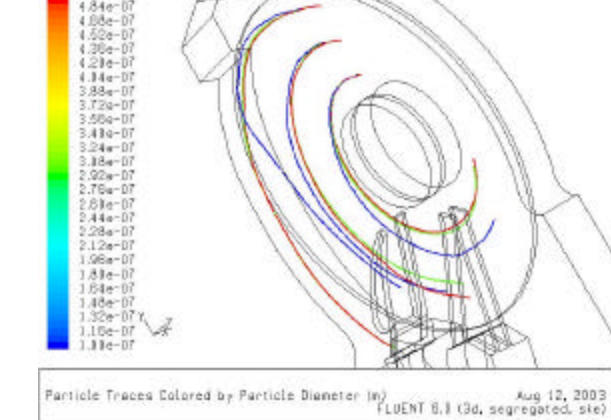
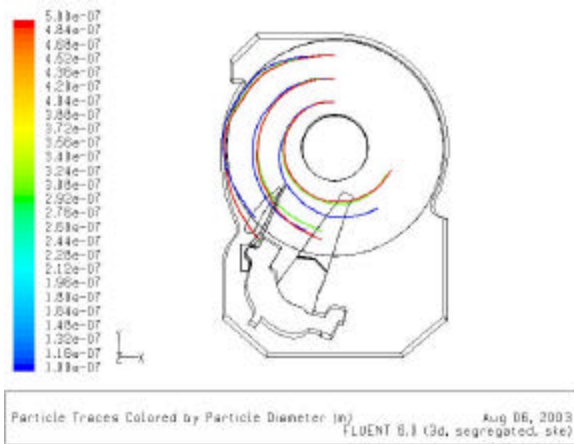


Fig. 11: Titanium Particle Tracks injected from Various Locations

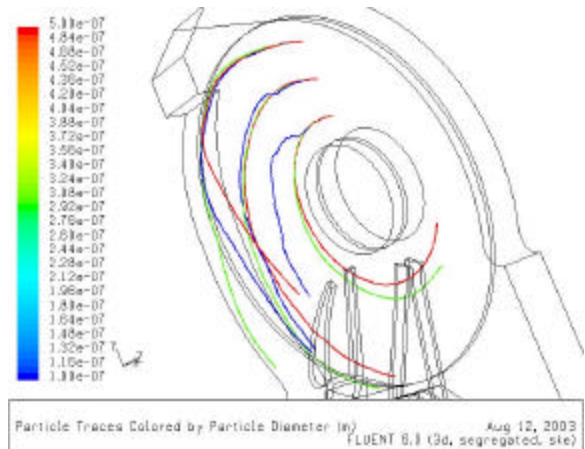
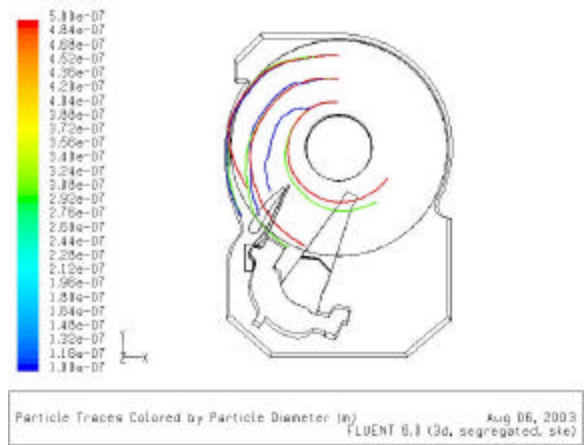
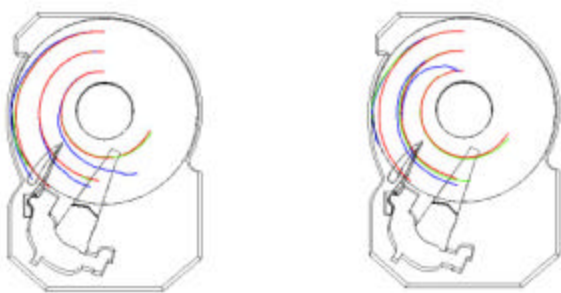


Fig. 12 Polystyrene Particle Tracks injected from Various Locations

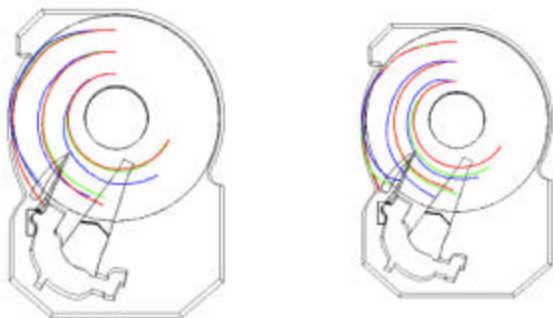
It can be seen that particles of different sizes follow different trajectories even though they are injected from the same position. This is because their mass is different in that their sizes are varied whereas the density is the same. Particles of different sizes will have different accelerations when subjected to the same external force. For example, in Fig. 14, the 0.1um particle injected from the ID flies to OD while particles of size 0.3um and 0.5um particles fly in the region between the ID and MD. The particle may change its velocity, because it is subjected to various forces in the trajectory. It can also be seen that titanium and polystyrene particles follow different paths although their sizes and injection positions are the same because of different densities. Based on the investigation, the trajectory tends to be different according to sizes and materials.

Fig. 13 compares the thermal effects on the alteration of the particle trajectories based on the same conditions considered earlier are considered for different rotating speeds at 3600RPM, 5400RPM, 7200RPM and 15000RPM.

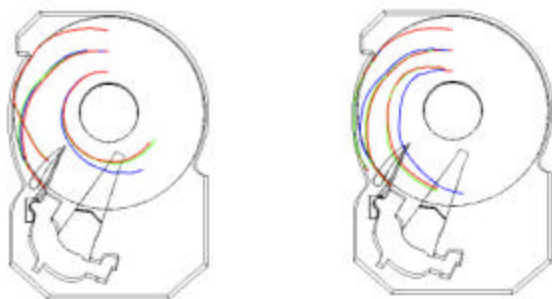
Simulation without Thermal Effects Simulation with Thermal Effects



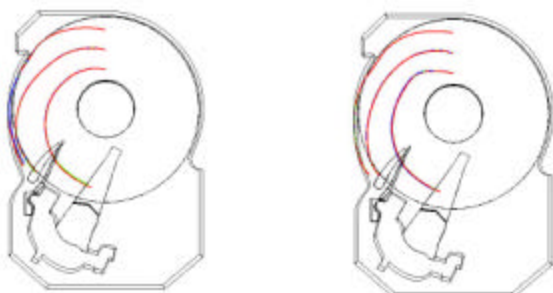
(a) 3600RPM



(b) 5400RPM



(c) 7200RPM



(d) 15000 RPM

Fig. 13: Computed Particles Trajectories corresponding to Different Disk RPMs with and without incorporating thermal effects

When the disk is rotating at 3600RPM, the smallest particle injected from the ID moves closely with other particles for a while, and then diverges in the vicinity of the MD, in the absence of thermal effects. However when thermal effects are factored in, it appears that the smallest particle injected from

the ID moves to the MD almost immediately. For the cases when the disk is rotating at 5400RPM and 7200RPM, the particles injected from one position diverge much further away from each other in the presence of thermal effects. When the disk is rotating at 15000RPM, the particles trajectory depends on their initial locations and move in clusters irrespective of particle sizes.

V. CONCLUSION

The airflow field inside a HDD enclosure has been computed using three turbulence models, namely the standard $k - \epsilon$, RNG $k - \epsilon$ and Reynolds Stress Method. By comparing the results, it appears that there are no major differences in the results from these three models. Considering the computing time and memory, it appears that the RNG $k - \epsilon$ model is the most appropriate and economical turbulent model for the airflow simulation in HDD. For engineering applications, this is more than sufficient to obtain the desired results. However, at higher RPMs such as 7200RPM and above, RNG $k - \epsilon$ could not converge to the stringent convergence criteria of 10^{-5} reduction in residuals. This difficulty may be due to the instability caused by high rotational speed. Standard $k - \epsilon$, on the other hand, converges to the same criteria more quickly no matter how high the rotating speed is. It is also observed that as rotational speeds of the disk increases, more iteration are required for the standard $k - \epsilon$ to converge. The velocity and the pressure contours appear similar no matter how high the rotating speed is. Incorporation of thermal effects enables one to investigate how the velocity and pressure field altered as a result of a heat source in a HDD. These models also enable the study the geometric effects of different 'flow modifiers'. By injecting particles of different sizes and materials at different locations, the particle trajectories were found to be dependent on the size and material properties. Lightweight particles tend to fly to the OD of the disk quickly. The particle trajectories can also change when thermal effects are considered. For very large rotating speeds of the disk it appears that the particle trajectories are all directed towards the outer regions of the disk.

This study will form the basis for additional further investigations. Prospects for further investigation are plentiful. As an example, thorough particle trajectory estimation will be done using user-defined functions. A more thorough study will be done to study more realistic thermal effects in the HDD. The steady flow field computed in this work will also form the basis for unsteady flow simulation. For example, the actuator arm may be moved in a defined manner, and the resulting unsteady flow field can be tracked with time to assess various effects of the airflow. Large Eddy Simulation (LES) models for turbulence will be used to predict the airflow. Estimates of shear stress field and airflow induced forces acting on the various components of the HDD may also be included.

REFERENCES

- [1] B. Bhushan and S. Chandra, "Detection and Sizing of Particulate Contamination in Rigid Disk Drives: Instruments and Sampling Techniques," IEEE Transactions on Magnetics, Vol.35, No.2, March 1999.
- [2] K.J. Ma, C.L. Chao, D.S. Liu, Y.T. Chen, M.B. Chieh, "Friction and Wear Behavior of TiN/Au, TiN/MoS₂ and TiN/TiCN/a-C:H Coatings," Journal of Materials Processing Technology Vol. 127, pp. 182-186, 2002.
- [3] L. Wu and D. B. Bogy, "Numerical Simulation of the Slider Air Bearing Problem of Hard Disk Drives by Two Multidimensional Upwind Residual Distribution Schemes over Unstructured Triangular Meshes," Journal of Computational Physics Vol. 172, pp. 640-657, 2001.
- [4] M. Tatewaki, N. Tsuda, T. Maruyama, "A Numerical Simulation of Unsteady Airflow in HDDs," FUJITSU Sci. Tech. J., Vol. 37, No.2, pp.227-235, December 2001.
- [5] FLUENT 6.0 User's Guide, Fluent Inc. USA, 2001.
- [6] Gambit 2.0 User's Guide, Fluent Inc. USA, 2001.